Desalination and Water Treatment
www.deswater.com

doi: 10.5004/dwt.2017.20254

64 (2017) 179–188
February

Removal of heavy metal ions by adsorption onto activated carbon prepared from *Stipa tenacissima* leaves

N. Madani[a,b,*], N. Bouchenafa-Saib[a], O. Mohammedi[a], F.J. Varela-Gandía[c], D. Cazorla-Amorós[c], B. Hamada[b], O. Cherifi[b]

[a]*Laboratoire de chimie physique des interfaces des matériaux appliqués à l'environnement, Faculté de Technologie Université Blida 1, B.P. 270 route de Soumaa, Blida 09000, Algérie, Tel. +213 561 264 323; Fax: +213 25 433 639; email: nesrine.madani@yahoo.fr (N. Madani), Tel. +213 555 487 804; Fax: +213 25 433 639; email: naima_bouchenafa@yahoo.fr (N. Bouchenafa-Saib), Tel. +213 554 657 843; Fax: +213 25 433 639; email: ourida.mohammedi@gmail.com (O. Mohammedi)*

[b]*Laboratoires synthèse pétrochimique, Université M'hamed Bougara, Avenue de l'Indépendance, Boumerdès 35000, Algérie, Tel. +231 552 407 912; Fax: +213 24816 848; email: bou.hamada@yahoo.fr (B. Hamada), Tel. +213 661 654 305; Fax: +213 24 816 086; email: ouizac@yahoo.fr (O. Cherifi)*

[c]*Departamento de Química Inorgánica e Instituto de Materiales, Universidad de Alicante, Ctra. San Vicente del Raspeig s/n, Ap. 99, E-03080 Alicante, Spain, Tel. +34 616 669 379; Fax: +34 965903454; email: fjvarelagandia@gmail.com (F.J. Varela-Gandía), Tel. +34 965 903 946; Fax: +34 965903454; email: cazorla@ua.es (D. Cazorla-Amorós)*

Received 18 September 2015; Accepted 16 October 2016

ABSTRACT

Biomass conversion into highly porous activated carbon (AC) materials is interesting particularly from the point of view of the reuse agricultural products. In this study, *Stipa tenacissima* leaves (STL) were used as precursor to prepare ACs by chemical activation method using phosphoric acid at different activation temperatures and a holding time of 1 h. The ratio of chemical activating agent to precursor was approximately 3:1. The effect of activation temperature on the textural properties of AC was studied. The optimum surface area obtained was 1,125 and 1,260 $m^2\ g^{-1}$ calculated using the Brunauer–Emmett–Teller equation and Langmuir equation, respectively. This AC, SAC 500, was tested in the adsorption of heavy metal ions from aqueous solutions, and the experimental conditions studied were contact time, pH and initial concentration, reaching the optimum experimental conditions. The adsorption experiments revealed relatively high adsorption kinetics, being the equilibrium time 90 min approximately, which follows the pseudo-second-order kinetic model. The Langmuir model provided the best fit to the experimental data. The thermodynamic parameters indicate that the adsorption process is spontaneous and endothermic. Bearing in mind these outstanding properties and the AC preparation methodology optimized, it is expected that an economical procedure for the treatment of wastewater can be obtained for the removal of heavy metal ions.

Keywords: Activated carbon; *Stipa tenacissima* leaves; Chemical activation; Heavy metals; Adsorption

1. Introduction

Water pollution caused by toxic heavy metal ions has been a major cause of concern for chemists and environmental engineers [1]. Heavy metal ions have long been recognized as ecotoxicological hazardous substances, and their chronic toxicities and accumulation abilities in living organism have been of great interest in the last years [2].

Apart from adsorption processes, there are several methods for water treatment, such as: filtration, ozonation, photocatalysis, membrane processes, electrocoagulation and

* Corresponding author.

chemical processes. However, the main drawbacks of these methods are high capital and operation costs or the disposal of the residual metal sludge [3]. The method under study is adsorption, which is a widely used process [4], due to its simplicity and easy operation conditions. Activated carbons (ACs) acting as adsorbents are widely used in the removal of heavy metal ions contaminants because of their excellent textural properties such as high micropore and mesopore volumes and surface area. However, commercially available ACs are expensive.

In the last years, there is a special interest in the preparation of ACs using as raw material agricultural by-products as a consequence of the growing interest in low-cost ACs production from renewable sources. These ACs could be especially prepared for applications related to wastewater treatment [5]. Thus, several studies deal with the preparation of AC using as raw materials: olive stones [6], date pits [7,8], fruit stones and nutshells [9] and bagasse [10], among others.

ACs preparation using lignocellulosic materials is carried out in two steps: (i) pyrolysis of the raw precursor to remove volatile matter and (ii) activation of the carbonized materials by physical or chemical activation treatment. Concerning physical activation, the carbonized precursor is activated in oxidizing atmosphere using steam, air or carbon dioxide [11] at selected activation conditions obtaining the final ACs [12]. In the case of the study of ACs preparation by chemical activation, the reaction is performed by using an activating agent such as phosphoric acid, potassium or sodium hydroxides, or zinc chloride, and the carbonization and activation are done, usually, in a single step. Finally, chemical activation presents several advantages compared with physical activation such as higher yield, less activation time and, generally, lower temperature of activation with higher development of porosity [13].

Dealing with the biomass precursor, it is considered as a natural renewable resource that can be converted into useful materials and energy [14]. The idea of using *Stipa tenacissima* leaves (STL) to produce AC rises in this context. *Stipa tenacissima*, also known as esparto grass, is a perennial grass grown in northwest Africa and the southern part of the Iberian Peninsula, which blooms between April and June. The leaves are cylindrical, tough and very tenacious reaching up to 1.5 m in height. Traditionally, esparto has been employed for crafts, such as cords and basketry, or for the production of paper. Humankind has used natural lignocellulosic materials since pre-history for an enormous amount of applications in daily life [15].

In this work, the results obtained on the preparation of ACs from STL with phosphoric acid activation at different temperatures are reported, and the capacity to remove Cd(II), Ni(II), Pb(II) and Zn(II) from dilute aqueous solutions has been studied. The influence of several operating parameters, such as contact time, pH of the solution and initial concentrations on the adsorption capacity, was investigated. The Langmuir and Freundlich models were used to analyze the adsorption equilibrium.

2. Materials and methods

2.1. Preparation of AC

STL precursor was washed several times with water and then dried at 110°C and, finally, milled and sieved, using the fraction of particle size between 0.5 and 1.0 mm for AC preparation.

The STL powder was impregnated with 2 mL of H_3PO_4 (85 wt%) per gram as proposed by Bouchenafa-Saib et al. [7], and the mixture was refluxed at 85°C during 3 h. Carbonization step was carried out in a quartz reactor at 500°C, 600°C and 700°C, with a heating rate of 10°C min^{-1}, during 1 h under nitrogen flow (100 mL min^{-1}). The prepared samples were named: SAC 500, SAC 600 and SAC 700, respectively. To eliminate the excess of H_3PO_4 in the AC sample, the ACs were washed in a Soxhlet extractor until a neutral pH was reached. The final ACs were dried at 110°C in an oven.

2.2. Characterization of AC

2.2.1. Characterization of porous texture

The measurement of the porosity of ACs produced from STL has been analyzed by nitrogen adsorption–desorption at –196°C isotherms, using an automatic adsorption system (Autosorb-6, Quantachrome). Before the adsorption experiments, the samples (about 0.2 g) were degassed at 200°C for 2 h under vacuum. Textural adsorption parameters were determined by applying the Brunauer–Emmett–Teller (BET) equation (S_{BET}) and *t*-plot method to obtain the micropore volume (V_μ).

2.2.2. Temperature-programmed desorption

The surface chemistry of the samples was analyzed by temperature-programmed desorption (TPD). About 10 mg of samples were heated from room temperature up to 900°C at a heating rate of 10°C min^{-1} in helium flow (200 cm^3 STP min^{-1}). The evolved gases from these experiments have been analyzed by mass spectrometry.

2.2.3. Point of zero charge

Point of zero charge (PZC) was determined by mass titration technique [16,17]. Initially, 50 cm^3 of 0.01 M NaCl solution was placed in a closed Erlenmeyer flask. The pH was adjusted to a value between 2 and 11 by adding HCl 0.1 M or NaOH 0.1 M solutions. Then, 0.15 g of each AC sample was added, and the final pH was measured after 48 h under agitation at room temperature. The pH_{pzc} is the point where the curve pH_{final} vs. pH_{inital} crosses the line $pH_{initial} = pH_{final}$.

2.2.4. Scanning electron microscopy

The surface texture resulting after activation has been examined by scanning electron microscopy (SEM). SEM was performed on a Philips XL30S-FEG cold field emission instrument. The accelerating voltage was 20 kV. Scanning was performed in situ on a carbon powder.

2.3. Batch adsorption studies

The SAC 500 was selected for the adsorption of Cd(II), Ni(II), Pb(II) and Zn(II) ions from aqueous solutions, because it has the optimum textural properties (see below). A known quantity of adsorbent (0.05 g) was added into 50 mL aqueous

solutions and stirred continuously. After the adsorption step, the aqueous phase was separated from the AC by centrifugation. Final metal ions concentration in the solutions were determined by atomic absorption spectroscopy (AAS), and the Fourier transform infrared (FTIR) spectra of the adsorbents before and after adsorption were recorded in the wave number range of 4,000–400 cm^{-1}. Metal adsorption capacity of AC was calculated by difference of initial and final solution concentration. The parameters under study were:

- contact time (5–240 min),
- initial concentration of heavy metal ions (10–100 mg L^{-1}), and
- pH of the solution (1–6), reaching the optimum parameters for metal adsorption process.

The amount of adsorption at equilibrium, Q_e (mg/g), was calculated by Eq. (1):

$$Q_e = \left(C_0 - C_e\right)\frac{V}{W} \quad (1)$$

where C_0 and C_e (mg L^{-1}) are the liquid-phase concentrations of heavy metal ions at initial and equilibrium, respectively. V is the volume of the solution (L) and W is the mass of dry adsorbent used (g). The percentage of removal of heavy metal ions was calculated from the Eq. (2):

$$R(\%) = \frac{C_0 - C_e}{C_0} \times 100 \quad (2)$$

3. Results and discussion

3.1. ACs characterization

The analysis of the textural characteristics of a given AC (BET surface area, micropore volume and total pore volume) is mandatory, and it has a strong influence in adsorption processes (i.e., removal of ion in water) [18]. Fig. 1 shows the nitrogen adsorption/desorption isotherms (–196°C) of the ACs prepared with different activation temperatures (500°C, 600°C and 700°C).

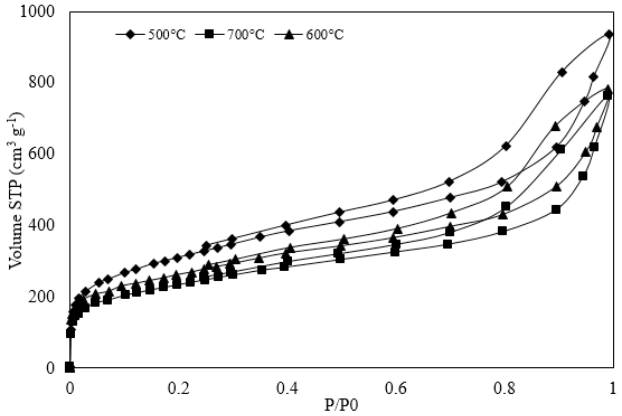

Fig. 1. Nitrogen adsorption–desorption isotherms at –196°C on the prepared activated carbons with H_3PO_4 at various pyrolysis temperatures 500°C, 600°C and 700°C.

In general, all the ACs prepared show modified type I isotherms with a type IV [19,20], corresponding to a well-developed microporous structure with a significant contribution of mesoporosity, which depends on the activationtemperature. The presence of mesopores is revealed by the slope of the isotherms at P/P_0 values over 0.25 and by the hysteresis cycles [21].

The N_2 volume adsorbed increases quickly at low relative pressure, which indicates micropore filling process [22]. The pore volume continues to progressively increase with the relative pressure with a sharp rise at high relative pressure. The progressive rise in pore volume indicates the availability of mesopores and the process of filling of the pores [21].

The textural properties (BET surface area, micropore, total pore volume and mesopore volumes) of the AC prepared from STL pyrolyzed at different activation temperatures under nitrogen are reported in Table 1.

The activation procedure carried out at 500°C was found to provide the highest BET surface area, 1,125 $m^2\ g^{-1}$, while the total pore volume is 1.45 $cm^3\ g^{-1}$. It is well known that the temperature of carbonization has an impact on the properties of the resulting ACs. Díaz-Teran et al. [12] observed that the required temperature for the development of the microporosity and a high specific surface area by phosphoric acid activation is between 400°C and 600°C. In our experiments, the surface area and micropore volume of the materials decreased with increasing the temperature from 500°C to 700°C, what is in agreement with previous results that showed that phosphoric acid treatment accelerates structural alteration at low temperatures [23]. In fact, it has been reported [24] that at temperatures above 500°C, the carbon structure shrinks, and the surface area decreases.

Above this temperature, the phosphate and polyphosphate bridges become unstable, producing chemical bond breakdown that causes the increase in size of aromatic units and a contraction in the AC material, which will result in a decrease of porosity [25].

Scanning electron micrographs of the surface morphology of the prepared ACs are given in Fig. 2. This figure shows that the adsorbent has an irregular surface characteristic of biomass.

TPD technique is used to characterize the carbon–oxygen surface groups, whose nature and amount depend on the starting material and the activation treatment [26,27]. According to Zhou et al. [28], surface oxygen complexes would decompose upon heating and release CO and/or CO_2 at different temperatures. In general, CO_2 evolution with the temperature results from carboxylic acids at low temperatures or lactones at high temperatures decomposition. Meanwhile, carboxylic anhydrides simultaneously decompose as CO and

Table 1
Textural characteristics of SACs

Samples	S_{BET} ($m^2\ g^{-1}$)	V_p total ($cm^3\ g^{-1}$)	$V_{\mu p}$ ($cm^3\ g^{-1}$)	V_{mesop} ($cm^3\ g^{-1}$)
SAC 500	1,125	1.45	0.45	0.48
SAC 600	935	1.21	0.37	0.38
SAC 700	840	1.18	0.33	0.33

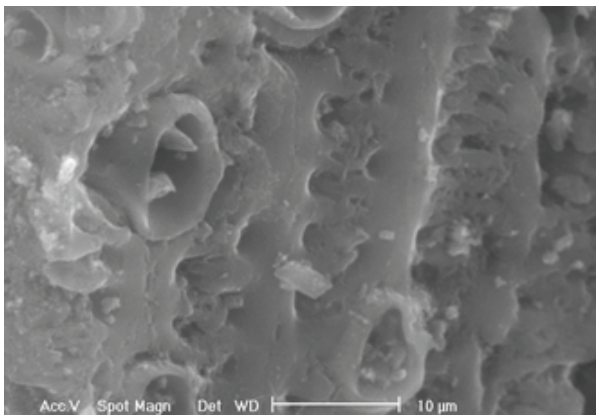

(a)

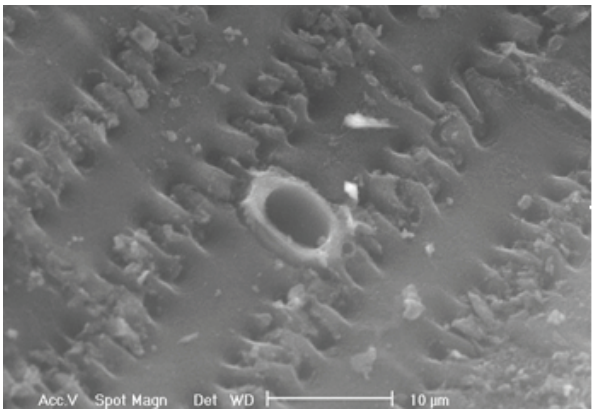

(b)

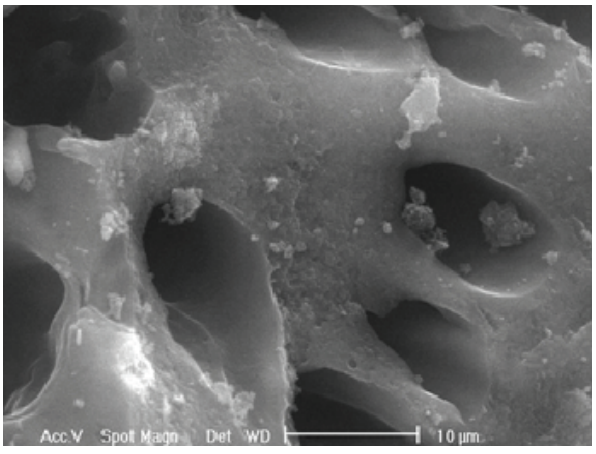

(c)

Fig. 2. SEM micrographs of the prepared activated carbon with H_3PO_4 at various pyrolysis temperatures: (a) 500°C, (b) 600°C and (c) 700°C.

CO_2. Finally, phenols, ethers and carbonyls groups decompose as CO molecules.

Figs. 3 and 4 show the TPD results that plot CO and CO_2 evolutions with temperature for the three prepared ACs. Table 2 summarizes the amounts of CO and CO_2 desorbed during the TPD of the ACs under study. Analyzing the CO evolution, all the ACs show a high increase in the

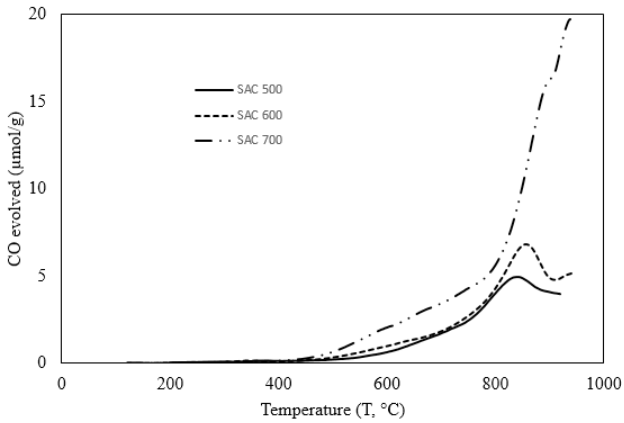

Fig. 3. CO evolution during the TPD of activated carbon.

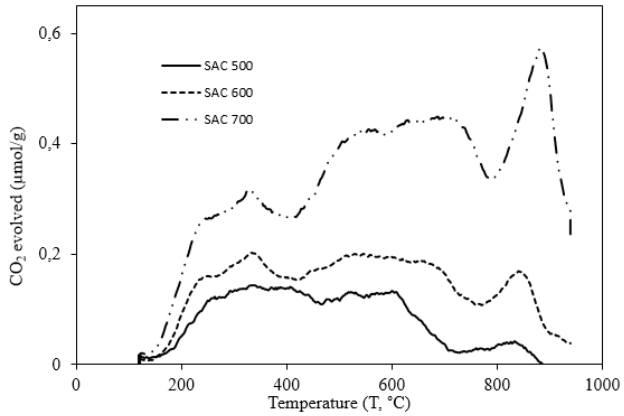

Fig. 4. CO_2 evolution during the TPD of activated carbon.

Table 2
CO and CO_2 evolved from TPD of activated carbons and the pH at the point of zero charge (PZC)

Samples	CO (µmol g^{-1})	CO_2 (µmol g^{-1})	Surface oxygen (wt%)	pH_{pzc}
SAC 500	2,970	193	5.37	5.50
SAC 600	3,934	352	7.40	6.30
SAC 700	8,003	832	15.47	8.10

CO evolution at temperatures between 800°C and 900°C. According to Rosas et al. [27], CO evolution at high temperatures can be related to the decomposition of P-surface groups formed during the phosphoric acid activation, such as relatively weak metaphosphates, C–O–PO_3 and C–PO_3 surface groups.

The amount of CO_2 evolved from the ACs is significantly lower than that corresponding to CO evolution, indicating a lower concentration of carboxyl, lactone and anhydride surface groups.

Fig. 5 shows the thermogravimetric analysis (TGA) curves for the prepared ACs. TGA curves show a weight loss assignable to release of moisture at around 120°C.

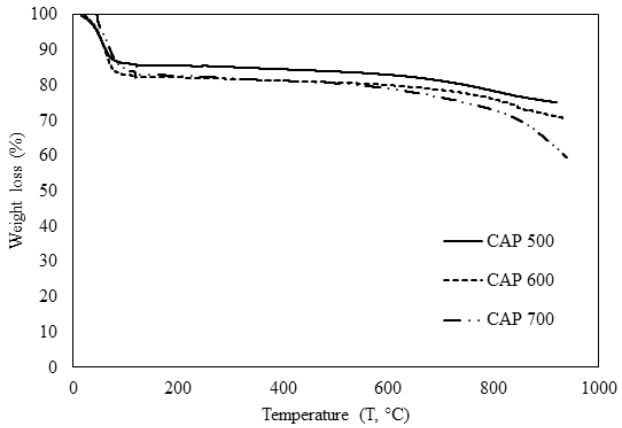

Fig. 5. Thermogravimetric analysis.

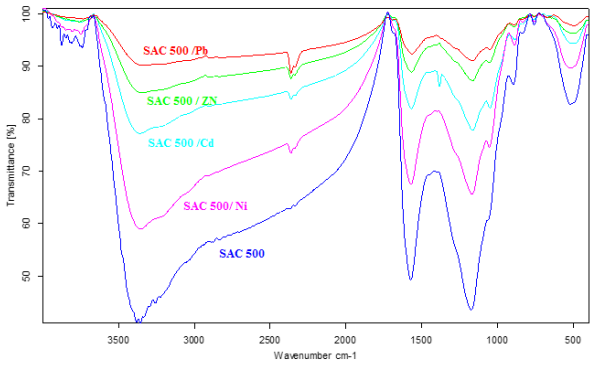

Fig. 6. FTIR spectra of SAC 500 before and after adsorption.

At temperatures close to 900°C, the weight loss will be nearly to 75.09%, 70.46% and 59.57% for SAC 500, SAC 600 and SAC 700, respectively, from the initial mass.

The pH at the PZC, pH_{PZC}, for the obtained ACs are also shown in Table 2. pH_{PZC} of an adsorbent is a very important property for adsorption in aqueous phase, since it defines the value where the surface of adsorbent is neutral, and beyond this pH, the adsorbent surface becomes either positively or negatively charged [29]. The ACs produced are effective adsorbents for removing the heavy metal cations at pH ≥ pH_{PZC}; since at these conditions, the surface will be negatively charged. According to the results exposed in Table 2, SAC 500 and SAC 600 have a slightly acidic surface (see pH_{pzc} values), which was expected due to the activation procedure applied, which caused the introduction of acidic groups based on phosphorus and other oxygen groups. Interestingly, a heat treatment at 700°C results in a weakly basic pH that can be related to the instability of phosphate and polyphosphate bonds.

The FTIR spectra of the SAC 500 before and after adsorption are shown in Fig. 6. The spectra display a number of absorption bands that can be assigned to various functional groups according to their respective wave numbers. Also, the bands for many functional groups shifted to different frequency levels indicating the possible involvement of those groups for adsorption of heavy metal ions.

The absorption spectrum showed broad bands between 3,200 and 3,600 cm^{-1} with a maximum at around 3,350 cm^{-1}, which indicates the presence of O–H in hydroxyl groups [3,15,29]. The peak at around 1,600 cm^{-1} could be assigned to the C–C stretching vibrations of polyaromatic C=C [20,28,29].

The strong band around 1,160 cm^{-1} with a shoulder around 1,050 cm^{-1} was observed. Assignment in this region may be difficult because absorption bands are overlapped. It is usually assigned to C–O stretching in acids, alcohols, phenols, ethers and/or esters group. Nevertheless, it is also a characteristic of phosphorus containing compounds present in the phosphoric acid ACs. Momčilović et al. [30] attributed the peak at 1,160 cm^{-1} to the stretching vibrations of hydrogen bonded P=O, stretching vibrations of O–C in P–O–C linkage, and P=OOH while the shoulder at 1,050 cm^{-1} could be assigned to the C–O–C stretching [15].

3.2. Effect of contact time on adsorption properties

The effect of contact time on removal of heavy metals by CAS 500 is summarized in Fig. 7. The study was performed at 25°C using a metal salt solution of 30 mg L^{-1}; pH was fixed at 6, and AC dose of 1 g L^{-1}.

It can be seen that the adsorption of Cd(II), Ni(II), Pb(II) and Zn(II) ions increased quite rapid initially and then gradually diminished to reach equilibrium after around 90 min for all metal ions studied. Similar trend was observed for adsorption of Cd(II) ions samples based on *Arundo donax* reed leaves used as adsorbent [31], Ni(II) and Mn(II) ions on montmorillonite [32], and Cd(II) adsorption onto untreated coffee grounds [33]. Rao et al. [34] have explained that the adsorption takes place rapidly on the external surface of the adsorbent.

3.3. Effect of the heavy metals concentration on adsorption properties

Heavy metal ions concentration in the solutions was established in the range of 10–100 mg L^{-1}. Fig. 8 shows the effect of initial concentration in the heavy metals ion removal capacity of SAC 500 sample. It has been shown that the removal yield decreases with the increase in initial heavy metal concentration. Also, Fig. 8 shows that the values of the adsorption capacity (Q_e) increase as the initial concentrations of metal ions increase. Several researchers [32–35] have explained that at low concentrations, metals are adsorbed by specific sites, while with increasing metal concentrations the specific sites are saturated at a certain concentration and the exchange sites are filled leading to less adsorption efficiency.

3.4. Effect of pH on adsorption properties

The interaction between the metal ions and the functional groups of the AC depends on nature of the adsorbent and the pH of the solution [34], which is one of the most important parameters affecting the adsorption process of metal ions.

Fig. 9 shows the effect of pH on heavy metals removal efficiencies of SAC 500. These studies were performed at a constant initial metal ions concentration of 30 mg L^{-1}, adsorbent quantity 1 g L^{-1} solution and agitation time of 90 min for all heavy metal ions. The required pH of solutions were adjusted by adding 0.1 M NaOH or 0.1 M HCl. It can be seen that the

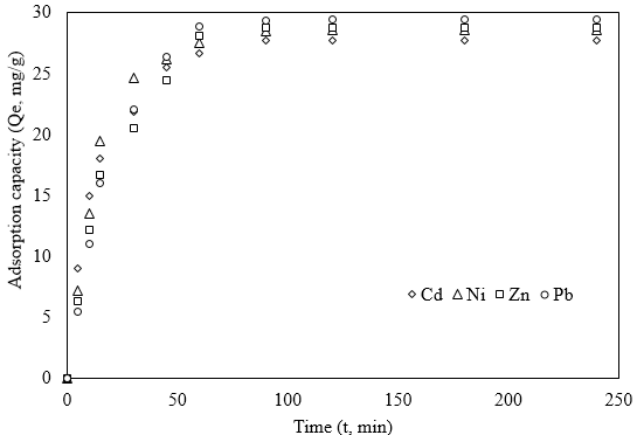

Fig. 7. Effect of contact time of Cd(II), Ni(II), Pb(II) and Zn(II) ions on removal: adsorbent dose 1 g L^{-1}, heavy metals concentration 30 mg L^{-1}, initial pH 6 and temperature 25°C.

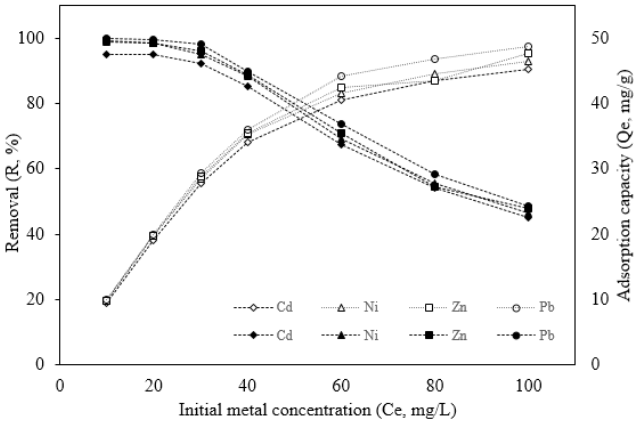

Fig. 8. Effect of initial concentration of Cd(II), Ni(II), Pb(II) and Zn(II) ions on removal: adsorbent dose 1 g L^{-1}, initial pH 6, time 90 min and temperature 25°C.

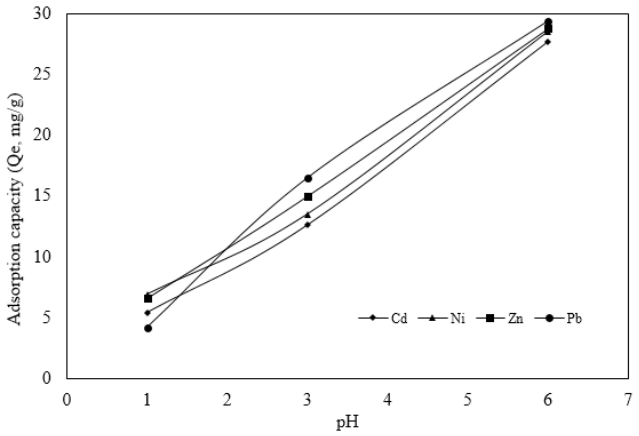

Fig. 9. Effect of pH of the solution of Cd(II), Ni(II), Pb(II) and Zn(II) ions on removal: adsorbent dose 1 g L^{-1}, heavy metals concentration 30 mg L^{-1}, time 90 min and temperature 25°C.

adsorption capacity increases with pH reaching a maximum at pH 6.0 with maximum removal of Cd(II), Ni(II), Pb(II) and Zn(II), which is obtained, 92.3%, 88.8%, 98% and 95.1%, respectively. Thereafter, it decreases with further increase in pH. This has been noticed by several researchers [31,36,37].

The increase in adsorption capacity with pH can be explained considering the pH_{pzc} of the SAC 500 (pH_{pzc} = 5.5, Table 2). At pH values much lower than pH_{pzc}, the surface of the SAC 500 is positively charged, resulting in an unfavored adsorption of cations due to electrostatic repulsion. On the other hand, Choi and Park [38] have studied the speciation for Cd(II), Ni(II), Pb(II) and Zn(II) from pH 5.0–11.0. They have reported that below pH 6.0, heavy metals are present predominantly as metal ions in the solution, which causes a competition between H^+ and M^{2+} ions for adsorption at the ion-exchangeable sites, leading to a low removal of metal. Similar findings have been reported by Meena et al. [35].

With increasing pH, the cations replaced hydrogen ions from the AC surface, and therefore, the adsorption extent will increase rapidly. It is probable that the carboxylic acid groups on the surface of SAC 500 are the main sites for the adsorption with the ion exchange of cations with the protons of carboxylic acid groups.

The speciation profile predicted that most of heavy metals are present as cations and no precipitation with anions occurs at pH 6.0 indicating that the removal of the metals is mainly accomplished by adsorption at this pH [35,38].

At the highest pH, the removal of metal ions takes place by adsorption as well as precipitation, due to formation of metal hydroxides. This can be explained by the fact that, as the pH of the solution increases, the concentration of OH^- ions in the solution increases and forms some complexes with metal ions and precipitates as metal hydroxides.

3.5. Adsorption isotherms

In order to describe the adsorption of Cd(II), Ni(II), Pb(II) and Zn(II) ions by SAC 500, the isotherms data were analyzed using three models: Langmuir, Freundlich and Dubinin–Radushkevich (D–R). The adsorption isotherm indicates how the molecules distribute between the liquid phase and the solid phase when the adsorption process reaches an equilibrium state. The analysis of the isotherm data by fitting them to different isotherm models is an important step to find the suitable model that can be used for design purposes [14].

3.5.1. Langmuir isotherm

The Langmuir model assumes that the uptake of metal ions occurs on a homogenous surface by monolayer adsorption without any interaction between adsorbed particles. Langmuir isotherm constants were calculated from the following linearized form:

$$\frac{C_e}{Q_e} = \frac{1}{Q_m b} + \frac{1}{Q_m} C_e \quad (3)$$

where C_e is the remaining concentration of adsorbate after equilibrium (mg L^{-1}), Q_e is the amount adsorbed at equilibrium (mg g^{-1}), and Q_m and b are Langmuir constants determined from the slope and intercept of the plot in Fig. 10,

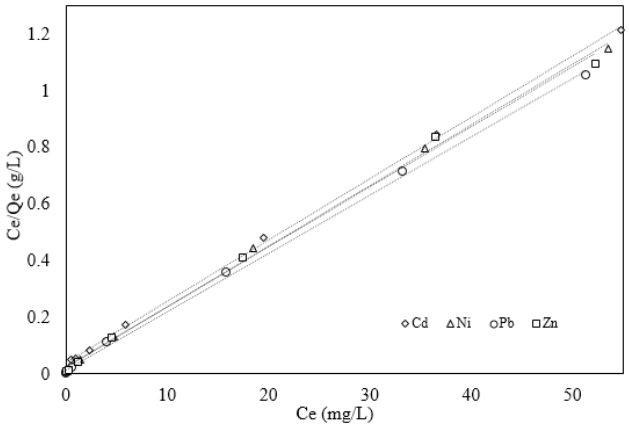

Fig. 10. The linearized Langmuir adsorption isotherms by SAC 500.

Table 3
Parameters of the linear representation of Langmuir, Freundlich and Dubinin–Radushkevich models at 25°C for the heavy metal ions adsorption onto SAC 500 (adsorbent dose: 1 g L^{-1}, initial pH 6 and time 90 min)

Model	Metal ion			
	Cd	Ni	Pb	Zn
Langmuir				
Q_m (mg g^{-1})	46.30	46.73	48.54	47.17
b (L mg^{-1})	0.52	0.98	1.42	0.95
R^2	0.999	0.999	0.999	0.997
Freundlich				
k_f	16.80	21.76	26.87	22.22
$1/n$	0.286	0.221	0.177	0.219
R^2	0.847	0.898	0.954	0.906
Dubinin–Radushkevich				
Q_m (mg g^{-1})	36.60	38.89	39.26	39.25
E (kJ mol^{-1})	1.58	3.53	7.07	3.53
R^2	0.946	0.928	0.881	0.930

indicative of maximum adsorption capacity (mg g^{-1}) of adsorbent and energy of adsorption, respectively.

The data related to the equilibrium obeyed well the Langmuir models. As seen from the values of regression coefficients presented in Table 3, the values of those are higher than 0.997, indicating the monolayer adsorption.

According to Özer and Pirincci [37], the essential characteristics of Langmuir isotherm can be explained in terms of a dimensionless constant separation factor (R_L), defined by Eq. (4):

$$R_L = \frac{1}{1 + bC_0} \tag{4}$$

where b is the Langmuir constant, and C_0 is the initial concentration of metal ion. The value of R_L indicated the type of Langmuir isotherm to be irreversible ($R_L = 0$), favorable ($0 < R_L < 1$), linear ($R_L = 1$) or unfavorable ($R_L > 1$) [30,31]. The values of R_L at 25°C decreased from 0.161 to 0.019 for Cd(II), from 0.092 to 0.010 for Ni(II), from 0.066 to 0.006 for Pb(II) and from 0.095 to 0.010 for Zn(II), while the initial concentration of all heavy metal ions concentration increased from 10 to 100 mg L^{-1}, which indicate that the adsorption of heavy metal ions is favorable on SAC 500.

3.5.2. Freundlich isotherm

Freundlich isotherm assumes that the uptake of metal ions occurs on a heterogeneous surface by multilayer adsorption and that the amount of adsorbate adsorbed increases infinitely with an increase in concentration. The Freundlich isotherm is expressed as:

$$Q_e = K_f \times C_e^{1/n} \tag{5}$$

where K_f and n are constants of Freundlich isotherm incorporating adsorption capacity (mg g^{-1}) and intensity, while C_e and Q_e are the remaining concentration of adsorbate after equilibrium (mg L^{-1}) and the amount adsorbed at equilibrium (mg g^{-1}), respectively. Eq. (5) is generally used in the linear form, represented by Eq. (6):

$$\log Q_e = \log K_f + \frac{1}{n}\log C_e \tag{6}$$

where K_f and n are the Freundlich adsorption constants, which can be determined by the linear plot of $\log Q_e$ vs. $\log C_e$. $1/n$ was found to be within the range of 0–1 (Table 3), indicating that the adsorption of heavy metal ions onto SAC 500 is favorable [14]. These results indicate the efficiency of the adsorbent under investigation.

3.5.3. D–R isotherm

The D–R isotherm does not assume a homogenous surface or a constant adsorption potential as the Langmuir isotherm and is given as:

$$Q_e = Q_m \exp\left(-B\,\varepsilon^2\right) \tag{7}$$

Eq. (7) can be expressed in linear form:

$$\ln Q_e = \ln Q_m - B\varepsilon^2 \tag{8}$$

where the saturation adsorption, Q_m, represents the total specific micropore volume of the sorbent. The value of B is related to the adsorption free energy, E (kJ mol^{-1}), which is defined as the free energy change required to transfer 1 mol of ions from solution to the solid surfaces [34], and ε is Polanyi potential, which is described as:

$$\varepsilon = \left[RT\,\ln\left(1 + \frac{1}{C_e}\right)\right] \tag{9}$$

where R is the ideal gas constant (8.31 J mol^{-1} K^{-1}), and T is the solution temperature (K). The value of mean adsorption energy, E (J mol^{-1}), can be calculated from D–R parameter B as follows:

$$E = \frac{1}{\sqrt{2B}} \tag{10}$$

The D–R constants were calculated from the linear plot of $\ln Q_e$ vs. ε^2, and the values are shown in Table 3. The R^2 values obtained for all heavy metal ions are low, which shows a poor fit to the experimental data.

Rao et al. [34] reported that the maximum adsorption capacity values of AC prepared from *Phaseolus aureus* hulls for metal ions were 21.8 mg g^{-1} for Pb(II), 21.2 mg g^{-1} for Zn(II), 19.5 mg g^{-1} for Cu(II) and 15.7 mg g^{-1} for Cd(II). Meena et al. [35] reported that the maximum adsorption capacity values of treated granular AC for metal ions were 0.75 mg g^{-1} for Pb(II), 45.62 mg g^{-1} for Hg(II), 400.8 mg g^{-1} for Cd(II), 561.7 mg g^{-1} for Cu(II), 1.275 mg g^{-1} for Mn(II), 1.843 mg g^{-1} for Zn(II) and 12.875 mg g^{-1} for Ni(II).

Özer and Pirincci [37] have investigated the adsorption of Cd(II) by using sulfuric acid-treated wheat bran (STWB). At pH 5.4, adsorption capacity for an initial Cd(II) ions concentration of 100 mg L^{-1} was found to be 43.1 mg g^{-1} at 25°C for contact time of 4 h. Whereas, the maximum Cd(II) adsorption capacity of *A. donax* leaves was reported by Ammari [31] as 27.9 mg g^{-1}. In another work, Özer [36] has investigated the adsorption of Pb(II) onto STWB. The adsorption percentage for an initial Pb(II) ions concentration of 100 mg L^{-1} was found to be 82.8 at 25°C for contact time of 2 h. Özer et al. [39] have reported also that the monolayer coverage capacity of *Enteromorpha prolifera* for Ni(II) ions was obtained as 65.36 mg g^{-1} at optimum biosorption temperature, 30°C, and initial pH, 5.0. While, the maximum Ni(II) adsorption capacity using waste of tea factory as adsorbent was reported to be 15.26 mg g^{-1} by Malkoc and Nuhoglu [40].

3.6. Adsorption kinetics

The pseudo-first-order kinetic model and pseudo-second-order kinetic model [33] were used to predict the mechanism involved in the adsorption process of Cd(II), Ni(II), Pb(II) and Zn(II) on SAC 500. The first-order equation can be expressed as:

$$\log\left(Q_e - Q_t\right) = \log Q_e - \left(\frac{k_1}{2.303}\right)t \tag{11}$$

where k_1 is the velocity constant of the pseudo-first-order (min^{-1}), which can be calculated by plotting $\log(Q_e - Q_t)$ vs. t. Q_t (mg g^{-1}) denotes the amount of the adsorption at time t (min), and Q_e (mg g^{-1}) is the amount of the adsorption at equilibrium. The pseudo-second-order equation can be written as:

$$\frac{t}{Q_t} = \frac{1}{(k_2 Q_e^2)} + \frac{t}{Q_e} \tag{12}$$

where k_2 is the velocity constant of the pseudo second order (g mg^{-1} min^{-1}). k_2 and Q_e can be obtained from the intercept and slope of plotting t/Q_t vs. t.

All kinetic data for the adsorption of ions onto SAC 500 calculated from the related plots are summarized in Table 4. The adsorption equilibrium was achieved in 90 min.

Since the correlation coefficients are closer to unity for pseudo-second-order kinetic model than for pseudo-first-order kinetic model according to Table 4, the adsorption kinetics can be well explained by pseudo-second-order kinetic model for the removal of Cd(II), Ni(II), Pb(II) and Zn(II) by the SAC 500.

3.7. Thermodynamic parameters

The thermodynamic parameters, such as free energy ($\Delta G°$), enthalpy change ($\Delta H°$) and entropy change ($\Delta S°$), were determined using the following equation:

$$\Delta G° = -RT\ln K_C \tag{13}$$

where R is the ideal gas constant (8.314 J mol^{-1} K^{-1}); T (K) is the absolute temperature and K_C is the thermodynamic equilibrium constant that is expressed as:

$$K_C = \frac{C_a}{C_e} \tag{14}$$

where C_a and C_s are the equilibrium concentration (mg L^{-1}) of the metal ion on adsorbent and in the solution, respectively.

The Gibb's free energy is also related to the $\Delta H°$ and $\Delta S°$ at constant temperature by the Van 't Hoff equation as follows:

$$\ln K_C = -\frac{\Delta G°}{RT} = -\frac{\Delta H°}{RT} + \frac{\Delta S°}{R} \tag{15}$$

The values of $\Delta H°$ and $\Delta S°$ were obtained from the slope and intercept of Van 't Hoff plots of $\ln K_C$ vs. $1/T$ as illustrated in Fig. 11, and the thermodynamic parameters are listed in Table 5.

The positive values of $\Delta H°$ indicate an endothermic process, which is supported by the increase in adsorption of all metal ions with the increase in temperature from 25°C to 50°C. Meena et al. [35] have suggested that the increase in adsorption with temperature may be attributed to the desolvation of the adsorbing species and the decrease in the thickness of the boundary layer surrounding the adsorbent with temperature, so that the mass transfer resistance of adsorbate in the boundary layer decreases. The $\Delta S°$ values are also positive that indicate an increase in randomness at the solid/solution

Table 4
Adsorption kinetics for removal of Cd(II), Ni(II), Pb(II) and Zn(II) by the SAC 500

Metal ion	Pseudo first order		Experiment	Pseudo second order		
	k_1 (min^{-1})	R^2	Q_{exp} (mg g^{-1})	Q_e (mg g^{-1})	k_2 10^3 (g mg^{-1} min^{-1})	R^2
Cd(II)	0.058	0.991	27.69	29.50	3.78	0.999
Ni(II)	0.051	0.986	28.53	30.03	3.83	0.998
Pb(II)	0.041	0.961	28.77	31.85	2.55	0.995
Zn(II)	0.040	0.936	29.40	30.86	2.25	0.997

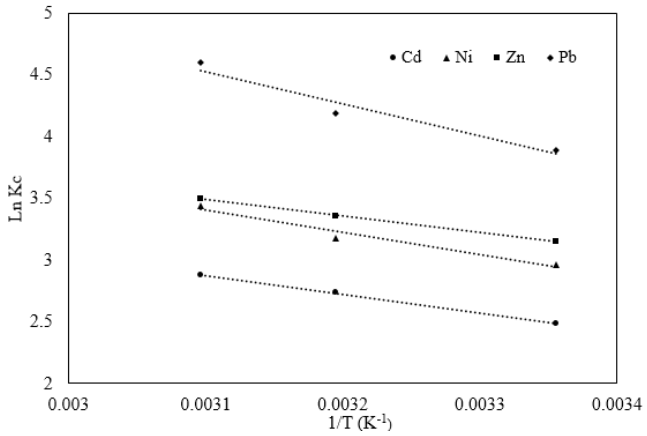

Fig. 11. Plot of $\ln K_C$ vs. $1/T$.

Table 5
Adsorption thermodynamic parameters

Metal	$\Delta H°$ (K mol^{-1})	$\Delta S°$ (J mol^{-1} K^{-1})	$-\Delta G°$ (KJ/mol)		
			298 K	313 K	323 K
Cd(II)	12.60	62.95	6.15	7.11	7.72
Ni(II)	14.84	74.29	7.34	8.27	9.24
Pb(II)	21.80	105.21	9.64	10.89	12.34
Zn(II)	10.38	61.07	7.81	8.74	9.38

interface during adsorption while low values of $\Delta S°$ indicate that the entropic change occuring from adsorption is not important. Similar results have been reported in previous works [32,35,36,40].

4. Conclusion

STL has been used to produce AC using a potentially inexpensive raw material coming from renewable resources. The AC, SAC 500, is a highly effective adsorbent. *Stipa tenacissima* is found in abundance in Algeria; then, carbon cost is expected to be economical.

AC produced from STL at relatively low temperatures can be tailored to reach the best combination of surface area and high surface concentrations of functional groups favorable for adsorption of positively charged metal species.

The adsorption of Cd(II), Ni(II), Pb(II) and Zn(II) onto SAC 500 was found to be highly influenced by initial concentration of metal ions and the initial solution pH, and the maximum adsoption capacity has been found at pH 6.

Adsorption data fitted well with the Langmuir, Freundlich and D–R models. However, Langmuir isotherm displayed a better fitting model because of the higher correlation coefficient that the former exhibited. Thus, indicating to the applicability of monolayer coverage of metal ions on the surface of adsorbent and adsorption capacity was found to be 46.30 mg g^{-1} for Cd(II), 46.73 mg g^{-1} for Ni(II), 48.54 mg g^{-1} for Pb(II) and 47.17 mg g^{-1} for Zn(II) at 25°C. The kinetics of heavy metal ions adsorption onto AC was based on the assumption of the pseudo-second-order mechanism. Thermodynamic constants were also evaluated using equilibrium constants changing with temperature. The negative value of $\Delta G°$ indicated the spontaneity, and the positive values of $\Delta H°$ and $\Delta S°$ showed the endothermic nature and irreversibility of heavy metal ions adsorption, respectively.

Acknowledgment

The authors thank the Ministry of Higher Education and Scientific Researches (MESRS) for the internship, and GV and FEDER for financial support (project PROMETEOII/2014/010).

References

[1] K. Mohanty, M. Jha, B.C. Meikap, M.N. Biswas, Removal of chromium (VI) from dilute aqueous solutions by activated carbon developed from *Terminalia arjuna* nuts activated with zinc chloride, Chem. Eng. Sci., 60 (2005) 3049–3059.
[2] F.N. Acar, Z. Eren, Removal of Cu(II) ions by activated poplar sawdust (Samsun clone) from aqueous solutions, J. Hazard. Mater., 137 (2006) 909–914.
[3] R. Vimala, N. Das, Mechanism of Cd(II) adsorption by macrofungus *Pleurotus platypus*, J. Environ. Sci., 23 (2011) 288–293.
[4] A. Üçer, A. Uyanik, Ş.F. Aygün, Adsorption of Cu(II), Cd(II), Zn(II), Mn(II) and Fe(III) ions by tannic acid immobilised activated carbon, Sep. Purif. Technol., 47 (2006) 113–118.
[5] M. Husseien, A.A. Amer, A. El-Maghraby, N.A. Taha, Utilization of barley straw as a source of a activated carbon for removal of methylene blue from aqueous solution, J. Appl. Sci. Res., 3 (2007) 1352–1358.
[6] J.M. Rosas, R. Ruiz-Rosas, J. Rodríguez-Mirasol, T. Cordero, Kinetic study of the oxidation resistance of phosphorus-containing activated carbons, Carbon, 50 (2012) 1523–1537.
[7] N. Bouchenafa-Saib, P. Grange, P. Verhasselt, F. Addoun, V. Dubois, Effect of oxidant treatment of date pit active carbons used as Pd supports in catalytic hydrogenation of nitrobenzene, Appl. Catal., A, 286 (2005) 167–174.
[8] F. Bouhamed, Z. Elouear, J. Bouzid, Adsorptive removal of copper(II) from aqueous solutions on activated carbon prepared from Tunisian date stones: equilibrium, kinetics and thermodynamics, J. Taiwan Inst. Chem. Eng., 43 (2012) 741–749.
[9] K.Y. Foo, B.H. Hameed, Preparation and characterization of activated carbon from pistachio nut shells via microwave-induced chemical activation, Biomass Bioenergy, 35 (2011) 3257–3261.
[10] K.A. Krishnan, K.G. Sreejalekshmi, R.S. Baiju, Nickel(II) adsorption onto biomass based activated carbon obtained from sugarcane bagasse pith, Bioresour. Technol., 102 (2011) 10239–10247.
[11] G. Cheng, L. Sun, L. Jiao, L.X. Peng, Z.H. Lei, Y.X. Wang, J. Lin, Adsorption of methylene blue by residue biochar from copyrolysis of dewatered sewage sludge and pine sawdust, Desal. Wat. Treat., 51 (2013) 7081–7087.
[12] J. Díaz-Teran, D.M. Nevskaia, A.J. López-Peinado, A. Jerez, Porosity and adsorption properties of an activated charcoal, Colloids Surf., A, 187 (2001) 167–175.
[13] M. Zabihi, A.H. Asl, A. Ahmadpour, Studies on adsorption of mercury from aqueous solution on activated carbons prepared from walnut shell, J. Hazard. Mater., 174 (2010) 251–256.
[14] B.H. Hameed, A.T.M. Din, A.L. Ahmad, Adsorption of methylene blue onto bamboo-based activated carbon: kinetics and equilibrium studies, J. Hazard. Mater., 141 (2007) 819–825.
[15] J.M. Valente Nabais, C. Laginhas, M.M.L. Ribeiro Carrott, P.J.M. Carrott, J.E. Crespo Amorós, A.V. Nadal Gisbert, Surface and porous characterisation of activated carbons made from a novel biomass precursor, the esparto grass, Appl. Surf. Sci., 265 (2013) 919–924.
[16] J.J.M. Órfão, A.I.M. Silva, J.C.V. Pereira, S.A. Barata, I.M. Fonseca, P.C.C. Faria, M.F.R. Pereira, Adsorption of a reactive dye on chemically modified activated carbons—influence of pH, J. Colloid Interface Sci., 296 (2006) 480–489.
[17] P.C.C. Faria, J.J.M. Órfão, M.F.R. Pereira, Adsorption of anionic and cationic dyes on activated carbons with different surface chemistries, Water Res., 38 (2004) 2043–2052.

[18] A.B.M. Noor, M.A.B.M. Nawi, Textural characteristics of activated carbons prepared from oil palm shells activated with $ZnCl_2$ and pyrolysis under nitrogen and carbon dioxide, J. Phys. Sci., 19 (2008) 93–104.
[19] K.S.W. Sing, Reporting physisorption data for gas/solid systems with special reference to the determination of surface area and porosity (Recommendations 1984), Pure Appl. Chem., 57 (1985) 603–619.
[20] Y. Chen, B. Huang, M. Huang, B. Cai, On the preparation and characterization of activated carbon from mangosteen shell, J. Taiwan Inst. Chem. Eng., 42 (2011) 837–842.
[21] W.C. Lim, C. Srinivasakannan, N. Balasubramanian, Activation of palm shells by phosphoric acid impregnation for high yielding activated carbon, J. Anal. Appl. Pyrolysis, 88 (2010) 181–186.
[22] D. Xin-hui, C. Srinivasakannan, W.W. Qu, W. Xin, P. Jin-hui, Z. Li-bo, Regeneration of microwave assisted spent activated carbon: process optimization, adsorption isotherms and kinetics, Chem. Eng. Process., 53 (2012) 53–62.
[23] M. Jagtoyen, M. Thwaites, J. Stencel, B. Mc Enaney, F. Derbyshire, Adsorbent carbon synthesis from coals by phosphoric acid activation, Carbon, 30 (1992) 1089–1096.
[24] A. Kriaa, N. Hamdi, E. Srasra, Removal of Cu (II) from water pollutant with Tunisian activated lignin prepared by phosphoric acid activation, Desalination, 250 (2010). 179–187.
[25] F. Suárez-Garcıa, A. Martınez-Alonso, J.M.D. Tascon, Pyrolysis of apple pulp: chemical activation with phosphoric acid, J. Anal. Appl. Pyrolysis, 63 (2002) 283–301.
[26] J.M. Rosas, J. Bedia, J. Rodríguez-Mirasol, T. Cordero, HEMP-derived activated carbon fibers by chemical activation with phosphoric acid, Fuel, 88 (2009) 19–26.
[27] J.M. Rosas, J. Bedia, J. Rodríguez-Mirasol, T. Cordero, Preparation of hemp-derived activated carbon monoliths. Adsorption of water vapor, Ind. Eng. Chem. Res., 47 (2008) 1288–1296.
[28] J.H. Zhou, Z.J. Sui, J. Zhu, P. Li, D. Chen, Y.C. Dai, W.K. Yuan, Characterization of surface oxygen complexes on carbon nanofibers by TPD, XPS and FT-IR, Carbon, 45 (2007) 785–796.
[29] A. Achmad, J. Kassim, T.K. Suan, R.C. Amat, T.L. Seey, Equilibrium, kinetic and thermodynamic studies on the adsorption of direct dye onto a novel green adsorbent developed from *Uncaria Gambir* extract, J. Phys. Sci., 23 (2012) 1–13.
[30] M. Momčilović, M. Purenović, A. Bojić, A. Zarubica, M. Ranđelović, Removal of lead(II) ions from aqueous solutions by adsorption onto pine cone activated carbon, Desalination, 276 (2011) 53–59.
[31] T.G. Ammari, Utilization of a natural ecosystem bio-waste; leaves of *Arundo donax* reed, as a raw material of low-cost eco-biosorbent for cadmium removal from aqueous phase, Ecol. Eng., 71 (2014) 466–473.
[32] K.G. Akpomie, F.A. Dawodu, K.O. Adebowale, Mechanism on the sorption of heavy metals from binary-solution by a low cost montmorillonite and its desorption potential, Alexandria Eng. J., 54 (2015) 757–767.
[33] N. Azouaou, Z. Sadaoui, A. Djaafri, H. Mokaddem, Adsorption of cadmium from aqueous solution onto untreated coffee grounds: equilibrium, kinetics and thermodynamics, J. Hazard. Mater., 184 (2010) 126–134.
[34] M.M. Rao, D.K. Ramana, K. Seshaiah, M.C. Wang, S.C. Chien, Removal of some metal ions by activated carbon prepared from *Phaseolus aureus* hulls, J. Hazard. Mater., 166 (2009) 1006–1013.
[35] A.K. Meena, C. Rajagopal, G.K. Mishra, G.K. Mishra, Removal of heavy metal ions from aqueous solutions using chemically (Na_2S) treated granular activated carbon as an adsorbent, J. Sci. Ind. Res., 69 (2010) 449–453.
[36] A. Özer, Removal of Pb(II) ions from aqueous solutions by sulphuric acid-treated wheat bran, J. Hazard. Mater., 141 (2007) 753–761.
[37] A. Özer, H.B. Pirincci, The adsorption of Cd (II) ions on sulphuric acid-treated wheat bran, J. Hazard. Mater., 137 (2006) 849–855.
[38] J. Choi, J.W. Park, Competitive adsorption of heavy metals and uranium on soil constituents and microorganism, Geosci. J., 9 (2005) 53–61.
[39] A. Özer, G. Gürbüz, A. Çalimli, B.K. Körbahti, Investigation of nickel(II) biosorption on *Enteromorpha prolifera*: optimization using response surface analysis, J. Hazard. Mater., 152 (2008) 778–788.
[40] E. Malkoc, Y. Nuhoglu, Removal of Ni(II) ions from aqueous solutions using waste of tea factory: adsorption on a fixed-bed column, J. Hazard. Mater., 135 (2006) 328–336.